Published as: *IETE J Res*. 2003 January 1; 49(2-3): 97–111.

Complex Cell-like Direction Selectivity through Spike-Timing Dependent Plasticity

RAJESH P N RAO and
Department of Computer Science and Neurobiology and Behavior Program, University of Washington, Seattle, WA 98195-2350 USA

TERRENCE J SEJNOWSKI
Howard Hughes Medical Institute, The Salk Institute for Biological Studies, 10010 N. Torrey Pines Road, La Jolla, CA 92037, USA and Department of Biology, University of California at San Diego, La Jolla, CA 92037, USA

RAJESH P N RAO: rao@cs.washington.edu; TERRENCE J SEJNOWSKI: terry@salk.edu

Abstract

Complex cells in primary visual cortex exhibit highly nonlinear receptive field properties such as phase-invariant direction selectivity and antagonistic interactions between individually excitatory stimuli. Traditional models assume that these properties are governed by the outputs of antecedent simple cells, but these models are at odds with studies showing that complex cells may receive direct inputs from the lateral geniculate nucleus (LGN) or can be driven by stimuli that fail to activate simple cells. Using a biophysically detailed model of recurrently connected cortical neurons, we show that complex cell-like direction selectivity may emerge without antecedent simple cell inputs, as a consequence of spike-timing dependent synaptic plasticity during visual development. The directionally-selective receptive fields of model neurons, as determined by reverse correlation and 2-bar interaction maps, were similar to those obtained from complex cells in awake monkey primary visual cortex. These results suggest a new interpretation of complex cells as integral components of an adaptive cortical circuit for motion detection and prediction.

Indexing terms

Neuroscience; Visual perception; Neural networks; Motion detection; Prediction

1. INTRODUCTION

In their seminal studies of cat and monkey visual cortex, Hubel and Wiesel classified neurons in the primary visual cortex as simple or complex based on their receptive field properties [1, 2]. Simple cells were identified as cells that are selective for stimulus orientation and phase, while complex cells were identified as those that respond to an oriented stimulus regardless of its position within the cell's receptive field. A majority of simple and complex cells are directionally-selective i.e. they respond best to oriented stimuli moving in a particular direction. Most complex cells are directionally-selective throughout their receptive fields, suggesting that their receptive fields are made up of directionally-selective sub-units. This led Hubel and Wiesel to suggest their well-known hierarchical model of visual processing in which on- and off-center cells in the LGN converge onto simple cells in the primary visual cortex, several of which in turn feed into a complex cell. Hubel and Wiesel's model has remained highly influential in guiding studies of the visual cortex and many elements of it have received experimental support [3,4].

However, several lines of evidence challenge the idea that complex cell outputs are determined solely by pooling the outputs of simple cells. First, there exists evidence for direct LGN input to complex cells without an antecedent simple cell stage [5–8]. In addition, several anatomical studies have suggested a lack of direct monosynaptic connections from simple to complex cells as postulated by the hierarchical model [9,10] (but see also [11]). These anatomical results are complemented by electrophysiological studies showing that certain classes of visual stimuli drive complex cells, but not simple cells [12–14]. Finally, many complex cells continue to exhibit responses when simple cells are silenced via pharmacological inactivation of corresponding input cells in the LGN, suggesting direct inputs to complex cells from the LGN [15].

These results suggest that there exists a class of complex cells that receive direct LGN inputs and whose outputs are not dependent on pooled simple cell inputs. What then is the source of the highly non-linear receptive field properties of these complex cells? One possibility is that the receptive field sub-units are computed within the dendritic tree of individual complex cells, as suggested by Mel and colleagues for orientation- and disparity-selective complex cells [16,17]. A similar single-neuron model for direction selectivity is possible [18], but as shown by Anderson *et al* [19], the biophysical properties of such a model can only account partially for the range of direction selective responses exhibited by cortical neurons.

Here, we pursue a second possibility, namely, that the source of the non-linear receptive field properties of complex cells is the pattern of excitatory and inhibitory connectivity in recurrent cortical networks. This pattern of connectivity may emerge as a consequence of spike-timing dependent plasticity in cortical circuits specialized for motion detection. Motivation for such a model comes from two fronts: (*a*) studies showing a strong influence of early visual experience on the development of direction selectivity [20,21], and (*b*) recent results suggesting an anatomical asymmetry between excitation and inhibition in direction-selective circuits in primary visual cortex [22].

We first show, using a detailed biophysical model of a recurrent cortical network, that an asymmetric pattern of intracortical connections can develop as a consequence of temporally asymmetric spike-timing dependent plasticity. Such a form of synaptic plasticity has been observed in recurrent cortical synapses [23], and in the hippocampus [24,25], the tectum [26], and in layer II/III of rat somatosensory cortex [27]. It has been shown to be useful for learning and predicting temporal sequences [28,29]. We show that a network of recurrently connected complex cells can develop non-linear directionally-selective receptive fields as a consequence of learning to predict moving stimuli. Space-time response plots of model complex cells to single flashed bars were found to be similar to those of complex cells in awake monkey VI.

Furthermore, the types of non-linear interactions observed in awake monkey complex cells due to pairs of successively flashed bars were also observed in the model and could be explained on the basis of the learned pattern of excitatory and inhibitory connections. These results suggest a new interpretation of complex cells in the visual cortex, namely, that they are vital components of an adaptive cortical circuit geared towards motion detection and prediction. Preliminary reports of this study appeared as [30] and [31].

1.1. Experimental Results

For our simulations, we used a two-compartment model of a cortical neuron consisting of a dendrite and a soma-axon compartment, as depicted in Fig 1*a*. The compartmental model was based on a previous study that demonstrated the ability of such a model to reproduce a range of cortical response properties [32]. Figure 1*a* illustrates the response of the model neuron to random excitatory and inhibitory Poisson-distributed synaptic inputs to the dendrite (see

Methods). The presence of voltage-activated sodium channels in the dendrite allowed backpropagation of action potentials from the soma into the dendrite as shown in Fig 1*b*. These backpropagated action potentials allowed the calculation of synaptic modifications as a function of local changes in membrane potential, as discussed below.

1.2. Simulating Spike-Timing Dependent Plasticity

Synaptic currents in the model were calculated using a kinetic model of synaptic transmission [33] with model parameters fitted to whole-cell recorded AMPA (α-amino-3-hydroxy-5-methyl-4-isoxazole proprionic acid) currents (see Methods for more details). Other inputs representing background activity were modeled as sub-threshold excitatory and inhibitory Poisson processes with a mean firing rate of 3 Hz. Synaptic plasticity was simulated by incrementing or decrementing the value for maximal synaptic conductance by an amount proportional to the temporal-difference in the postsynaptic membrane potential at time instants $t + \Delta t$ and $t - \Delta t$ for presynaptic activation at time t; this simulates a "temporal-difference" learning rule for prediction and yields asymmetric learning windows similar to those observed physiologically (see [29] for more details). Figure 1*c* shows the temporally asymmetric learning window observed in the model when the delay parameter Δt was set to 5 ms. In this case, potentiation was observed for EPSPs that occurred between 1 and 12 ms before the postsynaptic spike, with maximal potentiation at 6 ms. Maximal depression was observed for EPSPs occurring 6 ms after the peak of the postsynaptic spike and this depression gradually decreased, approaching zero for delays greater than 10 ms. As in rat neocortical neurons [23], Xenopus tectal neurons [26], and cultured hippocampal neurons [24], a narrow transition zone (roughly 3 ms in the model) separated the potentiation and depression windows. Note that the exact duration of the potentiation and depression windows in the model can be adapted to match physiological data by appropriately choosing the temporal-difference parameter Δt and/or varying the distribution of active channels in the dendrite the synapse is located on. Alternately, following [34], one could directly use one of the physiologically observed learning windows. This choice yields results that are qualitatively similar to those presented here.

2. DEVELOPMENT OF DIRECTION SELECTIVITY THROUGH SPIKE-TIMING DEPENDENT PLASTICITY

To illustrate how direction selective receptive fields can emerge as a consequence of spike-timing dependent learning, we first simulated a simple motion detection circuit consisting of a single chain of nine recurrently connected excitatory cortical neurons (Fig 2*a*). Each neuron in the chain initially received symmetric excitatory and inhibitory inputs of the same magnitude (maximal synaptic conductance 0.003μS) from its preceding and successor neurons (Fig 2*b*, "Before Learning"). Excitatory and inhibitory synaptic currents were calculated using kinetic models of synaptic transmission based on properties of AMPA and $GABA_A$ (γ-aminobutyric acid A) receptors as determined from whole-cell recordings (see Methods). Neurons in the network were exposed to 100 trials of retinotopic sensory input consisting of moving pulses of excitation in the rightward direction (5 ms pulse of excitation at each neuron). These inputs, which approximate the depolarization caused by nonlagged retinotopic inputs from the LGN, were sufficient to elicit a spike from each neuron.

The effects of spike-timing dependent learning on the excitatory and inhibitory synaptic connections in the network are shown in Fig 2*b* ("After Learning"). There is a profound asymmetry in the developed pattern of excitatory connections from the preceding and successor neurons to neuron 0 in Fig 2*b*. The synaptic conductances of excitatory connections from the left-side have been strengthened while the ones from the right-side have been weakened. This result can be explained as follows: due to the rightward motion of the input stimulus, neurons on the left side fire (on average) a few milliseconds before neuron 0 while neurons on the right

side fire (on average) a few milliseconds after neuron 0; as a result, the synaptic strength of connections from the left side are increased while the synaptic strength for connections from the right side are decreased, as prescribed by the spike-timing dependent learning window in Fig 1*c*. The opposite pattern of connectivity develops for the inhibitory connections because these were modified according to an asymmetric anti-Hebbian learning rule that reversed the polarity of the rule in Fig 1*c*. Such a rule is consistent with spike-timing dependent anti-Hebbian plasticity observed in some classes of inhibitory interneurons [35]. Alternatively, one could keep the level of inhibition constant (for example, at 0.015μS) and obtain qualitatively similar results because a decrease in the strength of the corresponding excitatory connections, as shown in Fig 2*b*, would again tilt the balance in favor of inhibition on the right side of neuron 0.

The responses of neuron 0 to rightward and leftward moving stimuli are shown in Fig 2*c*. As expected from the learned pattern of connections, the neuron responds vigorously to rightward motion but not to leftward motion. Similar responses selective for rightward motion were exhibited by other neurons comprising the network. More interestingly, each neuron fires a few milliseconds before the time of arrival of the input stimulus at its soma (marked by an asterisk) due to recurrent excitation from preceding neurons. Such predictive neural activity is characteristic of temporally asymmetric learning rules (see, for example, [28;29]). In contrast, motion in the non-preferred direction triggered recurrent inhibition and little or no response from the model neurons.

2.1. Detecting Multiple Directions of Motion

To investigate the question of how selectivity for different directions of motion may emerge simultaneously, we simulated a network comprised of two parallel chains of neurons (see Fig 3*a*), each containing 55 neurons, with mutual inhibition (dark arrows) between corresponding pairs of neurons along the two chains. As in the previous simulation, a given excitatory neuron received both excitation and inhibition from its predecessors and successors, as shown in Fig 3*b* for a neuron labeled '0'. Inhibition at a given neuron was mediated by an inhibitory interneuron (dark circle) which received excitatory connections from neighboring excitatory neurons (Fig 3*b*, lower panel). The interneuron received the same input pulse of excitation as the nearest excitatory neuron. Maximum conductances for all synapses were initialized to small positive values (dotted lines in Fig 3*c*). To break the symmetry between the two chains, one may: (*a*) select small randomly chosen values for the synaptic conductances in the two chains, or (*b*) provide a slight bias in the recurrent excitatory connections, so that neurons in one chain may fire slightly earlier than neurons in the other chain for a given motion direction. Both alternatives succeed in breaking symmetry during learning. We report here the results for alternative (*b*), which is supported by experimental evidence indicating the presence of a small amount of initial direction selectivity in cat visual cortical neurons before eye opening [36].

To evaluate the consequences of synaptic plasticity in the two-chain network, model were exposed alternately to leftward and rightward moving stimuli for a total of 100 trials. The excitatory connections (labeled 'EXC' in Fig 3*b*) were modified according to the asymmetric Hebbian learning rule in Fig 1*c* while the excitatory connections onto the inhibitory interneuron (labeled 'INH') were modified according to the asymmetric anti-Hebbian learning rule, as in the previous simulation. The synaptic conductances learned by two neurons (marked N1 and N2 in Fig 3*a*) located at corresponding positions in the two chains after 100 trails of exposure to the moving stimuli are shown in Fig 3*c* (solid line). The excitatory and inhibitory connections to neuron N1 exhibit a marked asymmetry, with excitation originating from neurons on the left and inhibition from neurons on the right. Neuron N2 exhibits the opposite pattern of connectivity.

As expected from the learned pattern of connectivity, neuron N1 was found to be selective for rightward motion while neuron N2 was selective for leftward motion (Fig 3*d*). Moreover, when

stimulus motion is in the preferred direction, each neuron starts firing a few milliseconds before the time of arrival of the input stimulus at its soma (marked by an asterisk) due to recurrent excitation from preceding neurons. Conversely, motion in the non-preferred direction triggers recurrent inhibition from preceding neurons as well as inhibition from the active neuron in the corresponding position in the other chain. Thus, the learned pattern of connectivity allows the direction selective neurons comprising the network to conjointly code for and predict the moving input stimulus in each possible direction of motion.

To test the importance of temporal order of spikes in learning direction selectivity, we investigated whether classical rate-based Hebbian learning [37] could also lead to a similar pattern of asymmetry in connections and produce direction selectivity in our network. In rate-based Hebbian learning, a connection between two neurons is strengthened based on the correlation between the firing rates of the two neurons, irrespective of the temporal order of input and output spikes. We used the same network as in the previous simulation (see Fig 3*a* and 3*b*, and Fig 4 - top panel), with an identical initial bias in the network connectivity as shown in Fig 3*c* (dotted lines). The network was exposed to 100 trials of rightward and leftward moving stimuli as before, but a rate-based Hebbian learning rule was used for modifying the synaptic conductances. In particular, conductances for connections onto excitatory (inhibitory) neurons were increased (decreased) based on correlations between pre- and postsynaptic spikes within a 30 ms temporal window regardless of the temporal order of the spikes. As shown in Fig 4 (middle panel), despite the initial bias in connectivity, the network fails to develop asymmetric connections using the purely rate-based Hebbian learning rule. Neurons in the two chains were found to respond similarly to both leftward and rightward moving input stimuli, demonstrating a failure to develop direction selectivity (Fig 4, bottom panel). These results suggest that spike-timing dependent learning mechanisms may play a crucial role in sculpting and maintaining direction-selective circuits in the visual cortex.

3. THE IMPORTANCE OF RECURRENT EXCITATORY AND INHIBITORY CONNECTIONS

To investigate the role of recurrent excitation in the model, we gradually decreased the value of the maximum synaptic conductance between excitatory neurons in the trained network of Fig 3, starting from 100% of the learned values. For a stimulus moving in the preferred direction, decreasing the amount of recurrent excitation increased the latency of the first spike in a model neuron and decreased the spike count until, with less than 10% of the learned recurrent excitation, the latency equaled the arrival time of the input stimulus and the spike count dropped to 1 (Fig 5*a* and 5*b*). These results illustrate the role of recurrent excitation in generating predictive activity in the network and in enhancing direction selective responses by increasing the spike count in the preferred direction.

To evaluate the role of inhibition in maintaining direction selectivity in the model, we quantified the degree of direction selectivity using the direction index: 1 -(Number of Spikes in Non-Preferred Direction)/(Number of Spikes in Preferred Direction). Direction indices were calculated for a trained network consisting of two chains of neurons, each containing 35 excitatory and 35 inhibitory neurons. Figures 5*c* and 5*d* show the distribution of direction indices with and without inhibition in the network. In the control case, most of the excitatory neurons and inhibitory interneurons receiving recurrent excitation are highly direction selective. Blocking inhibition significantly reduces direction selectivity in the model neurons but does not completely eliminate it, consistent with some previous physiological observations [38, 39]. The source of this residual direction selectivity in the absence of inhibition can be traced to the asymmetric recurrent excitatory connections in the model network which remain unaffected by the blockage of inhibition.

3.1. Comparison to Awake Monkey Complex Cell Responses: First-Order Analysis

Similar to complex cells in primary visual cortex, model neurons were found to be direction selective throughout their receptive field. This phase-invariant direction selectivity is a consequence of the fact that at each retinotopic location, the corresponding neuron in the chain receives the same pattern of asymmetric excitation and inhibition from its neighbors as any other neuron in the chain. Thus, for a given neuron, motion in any local region of the chain will elicit direction selective responses due to recurrent connections from that part of the chain. This is consistent with previous modeling studies [40] suggesting that recurrent connections may be responsible for the spatial-phase invariance of complex cell responses.

The model predicts that the neuroanatomical connections for a direction selective neuron should exhibit a pattern of asymmetrical excitation and inhibition similar to Fig 3*c*. A recent study of complex cells in awake monkey V1 found excitation on the preferred side of the receptive field and inhibition on the null side, consistent with the pattern of connections learned by the model [18]. In this study, optimally oriented bars were flashed at random positions in a cell's receptive field, and a reverse correlation map was calculated from a record of eye position, spike occurrence, and stimulus position. Fig 6 (top panel, left) depicts an eye-position corrected reverse correlation map for a complex cell, with time on the *x*-axis and stimulus position on the *y*-axis: each row of the map is the post-stimulus time histogram of spikes elicited for a bar flashed at that spatial position. The map thus depicts the firing rate of the cell as a function of the retinal position of the stimulus and time after stimulus onset.

For comparison with these experimental data, spontaneous background activity in the model was generated by incorporating Poisson-distributed random excitatory and inhibitory alpha synapses on the dendrite of each model neuron. As shown in Fig 6 (top panel), there is good qualitative agreement between the space-time response plot for the direction-selective complex cell and that for the model. Both space-time plots show a progressive shortening of response onset time and an increase in response transiency going in the preferred direction: in the model, this is due to recurrent excitation from progressively closer cells on the preferred side. Firing is reduced to below background rates 40–60 ms after stimulus onset in the upper part of the plots: in the model, this is due to recurrent inhibition from cells on the null side. The response transiency and shortening of response time course appears as a slant in the space-time maps, but unlike space-time maps in simple cells, this slant cannot be used to predict the neuron's velocity preference (see [18] for more details). However, assuming a 200 μm separation between excitatory model neurons in each chain and utilizing known values for the cortical magnification factor in monkey striate cortex [41], one can estimate the preferred stimulus velocity of model neurons to be in the range of 3.1°/s in the fovea and 27.9°/s in the periphery (at an eccentricity of 8°), which is within the range of monkey V1 velocity preferences (1°/s to 32°/s) [18,42].

3.2. Comparison to Awake Monkey Complex Cell Responses: Second-Order Analysis

Complex cells are known to exhibit higher-order interactions between two successively presented stimuli. For example, the response to two oriented bars presented sequentially at two different positions is generally not a linear function of the responses to the bars presented individually. In the case of the model network, we would expect the asymmetry in synaptic connections to give rise to non-linear facilitation if the two bars are flashed along the preferred direction relative to each other and a reduction in response for bars flashed in the opposite direction (see Fig 7*a*).

To study such 2-bar interactions in complex cells in awake monkey V1, single bars of optimal orientation were flashed within a direction selective cell's receptive field at a series of locations along the dimension perpendicular to stimulus orientation (these experiments were conducted

in Margaret Livingstone's laboratory at Harvard Medical School). A continuous record was kept of eye position (at 250 Hz), spike occurrence (1 ms resolution), and stimulus position. A reverse correlation analysis was performed, after correcting for eye position, to produce two-bar interaction maps as shown in Fig 7b. These maps show how the response to one stimulus is influenced by a preceding stimulus, as a function of the two stimulus locations. Thus, for each of the plots shown, the *y*-axis represents the spatial position of bar 1 while the *x*-axis represents the position of bar 2, which was flashed after an inter-stimulus-interval (ISI) of 56 ms after bar 1. The four plots represent the evolution of the cell's response to the two bar sequence at delays of 25 ms, 50 ms, 75 ms, and 100 ms respectively after the onset of bar 2. The average responses for the individual bars were subtracted from each of the plots to show any facilitation or reduction in responses due to sequential interactions.

Facilitation (red) can be observed above the diagonal line for all four plots in Fig 7*b*. Locations above the diagonal represent cases where the two bar sequence is flashed in the preferred direction of the cell (see Fig 7*a*). A reduction in the cell's response (blue) occurs at longer delays, predominantly at positions below the diagonal. This is consistent with the model predictions sketched in Fig 7*a*. A repetition of the two-bar experiment in the model yielded interaction plots that were qualitatively similar to the physiological data (Fig 7*c*). The main differences are in the time scale and magnitude of facilitation/reduction in the responses, both of which could be fine-tuned, if necessary, by adjusting model parameters such as the maximal allowed synaptic conductance, synaptic delays, and the number of neurons used in the simulated network.

4. CONCLUSIONS AND FUTURE WORK

Our results suggest that a network of cortical neurons can develop complex-cell-like receptive field properties as a consequence of spike-timing dependent plasticity in cortical circuits for motion detection. The model predicts that some direction selective complex cells should start responding a few milliseconds before the preferred stimulus arrives at the retinotopic location of the neuron in primary visual cortex. Such predictive neural activity has recently been reported in ganglion cells in the rabbit and salamander retina [43]; the extent to which neural responses in V1 can be characterized as being predictive remains an interesting open question.

The development of complex cell receptive fields in our model is activity-dependent and is based on the assumption that these receptive fields can be modified by visual experience, either directly via moving visual stimuli or indirectly via traveling waves in the developing retina. Such an assumption is consistent with experimental evidence indicating that visual experience during a critical period can profoundly affect the development of direction selectivity in the visual cortex. For example, direction selectivity in kittens can be influenced by selective exposure to a single direction of motion [20] and even abolished by strobe rearing [21]. Although several models for the development of direction selectivity have been proposed [44,45], the roles of spike timing and asymmetric Hebbian plasticity have not been previously explored. An interesting question currently being investigated is whether the explicit dependence of visual development on spike timing in our model can account for the fact that only low frequencies of stroboscopic illumination (approximately 8- Hz or below) cause a loss of direction selectivity.

In a recent study [22], Roerig and Kao showed, using a combination of *in vivo* and *in vitro* techniques, that excitatory synaptic inputs to direction selective cells in ferret primary visual cortex iso-direction tuned, emanating from local regions preferring the same direction of motion. On the other hand, up to 40% of the inhibitory connections originated in cortical regions preferring the opposite direction of motion. Such a distribution of synaptic inputs is consistent with the pattern of connections predicted by our model as a consequence of spike-timing

dependent plasticity. Whether the same anatomical result holds for macaque primary visual cortex remains an open question.

Several other models of cortical direction selectivity based on circuit-level interactions have previously been proposed [45–50]. Most of these have been aimed at capturing the properties of simple cells in layer IV of primary visual cortex in anesthetized cats. For example, Maex and Orban [48] and Suarez *et al* [50] present models for direction selectivity based on the idea of spatially asymmetric connectivity and intracortical amplification. Both of these are intended to be models of simple cell direction selectivity. The model analyzed by Mineiro and Zipser [49] is similar to our model, although at a more abstract level. None of the above models addresses the issue of how network connectivity may develop naturally as a consequence of synaptic plasticity. Wimbauer *et al* present a model for the development of direction selectivity in simple cells in cat striate cortex based on rate-based Hebbian learning and lagged/non-lagged inputs from the LGN [45]; however, the applicability of this model to monkey visual cortex is unclear given that there is inconclusive evidence for lagged/nonlagged cells in monkey LGN. A popular class of models that captures some important properties of complex cells is the class of spatiotemporal energy models [51,52]; these typically utilize the squared outputs of a pair of quadrature filters that model simple cell receptive fields. Although extremely useful as phenomenological models, such models would not be applicable to cases where a given complex cell receives direct non-oriented LGN inputs.

Temporally asymmetric Hebbian learning has previously been suggested as a possible mechanism for sequence learning in the hippocampus [28,25] and as an explanation for the asymmetric expansion of hippocampal place fields during route learning [53,54]. Some of these theories require relatively long temporal windows of synaptic plasticity (on the order of several hundreds of milliseconds) [28] while others have utilized temporal windows in the sub-millisecond range for coincidence detection [55]. Prediction and sequence learning in our model is based on a window of plasticity in the tens of milliseconds range which is roughly consistent with recent physiological observations [23,24,26,27]. Although a fixed learning window (roughly 15 ms of potentiation/depression) was used in the simulations, the temporal extent of this window can be modified by changing the parameter Δt. The model predicts that the shape and width of the asymmetric learning window should be a function of the backpropagating action potentials in the dendrite that the synapse is located on (see [29] for more details). In the case of hippocampal neurons and cortical neurons, the width of backpropagating action potentials in apical dendrites has been reported to be in the range of 10–25 milliseconds, which is comparable to the size of potentiation/depression windows for synapses located on these dendrites [24,56].

In *vitro* experiments involving cortical and hippocampal slices suggest the possibility of short-term plasticity in synaptic connections onto pyramidal neurons [57–59]. The kinetic model of synaptic transmission used in the present study can be extended to include short-term plasticity with the addition of a parameter governing the level of depression caused by each presynaptic action potential [40,57,59]. The adaptation of this parameter may allow finer control of postsynaptic firing in the model in addition to the coarse-grained control offered by modifications of maximal synaptic conductance. As suggested by previous studies [40,57], we expect the addition of synaptic depression in our model to enhance the transient response of model neurons to stimuli such as flashed bars (see Fig 6) and to broaden the response to drifting stimuli, due to the reduced sensitivity of postsynaptic neurons to mean presynaptic firing rates.

In summary, our results suggest the new hypothesis that complex cells may play a crucial role in predicting and tracking moving stimuli as part of an adaptive cortical network for motion detection. Prediction and sequence learning have both been previously suggested as important goals of cortical information processing [28,60–67]. Our biophysical simulations suggest a

specific mechanism for achieving these goals in the context of visual information processing. Given the discovery of spike-timing dependent learning mechanisms in several different cortical areas [23,25,27], the biophysical mechanisms investigated herein may prove useful in studying information processing in other cortical areas as well.

5. METHODS

5.1. Neocortical Neuron Model

Two-compartment model neocortical neurons consisting of a dendritic compartment and a soma-axon compartment [32] were implemented using the simulation software Neuron (M Hines, in Neural Systems: Analysis and Modeling, F H Eeckman, editor (Kluwer, Boston, MA, 1993), pp 127–136). Four voltage-dependent currents and one calcium-dependent current were simulated: fast Na^+, I_{Na}; fast K^+, I_{Kv}; slow non-inactivating K^+, I_{Km}; high voltage-activated Ca^{2+}, I_{Ca} and calcium-dependent K^+ current, $I_{K\,Ca}$ (see [32] for references). Conventional Hodgkin-Huxley-type kinetics were used for all currents (integration time step = 25 μs temperature = 37° celsius). Ionic currents I were calculated using the ohmic equation: $I = \bar{g}A^X B(V–E)$ where $\bar{g}$ is the maximal ionic conductance density, A and B are activation and inactivation variables respectively (x denotes the order of kinetics - see [32] for further details), and E is the reversal potential for the given ion species (E_K = −90 mV, E_{Na} = 60mV, E_{ca} = 140 mV, E_{leak} = −70 mV). The following active conductance densities were used in the dendritic compartment (in pS/μm^2): $\bar{g}_{Na}$= 20, $\bar{g}_{ca}$= 0.2, $\bar{g}_{Km}$= 0.1, and $\bar{g}_{K\,ca}$= 3, with leak conductance 33.3 μS/cm^2 and specific membrane resistance 30 kΩ-cm^2. The soma-axon compartment contained $\bar{g}_{Na}$ = 40,000 and $\bar{g}_{kv}$ = 1400. For all compartments, the specific membrane capacitance was 0.75 μF/cm^2. Two key parameters governing the response properties of the model neuron are [32]: the ratio of axosomatic area to dendritic membrane area (ρ) and the coupling resistance between the two compartments (κ). For the present simulations, we used the values ρ = 150 (with an area of 100 μm^2 for the soma-axon compartment) and a coupling resistance of $\kappa = 8\ M\ \Omega$. Poisson-distributed synaptic inputs to the dendrite were simulated using alpha function [68] shaped current pulse injections (time constant = 5 ms) at Poisson intervals with a mean presynaptic firing frequency of 3 Hz.

5.2. Model of Synaptic Transmission and Plasticity

Synaptic transmission at excitatory (AMPA) and inhibitory ($GABA_A$) synapses was simulated using first order kinetics of the form:

$$\frac{dr}{dt} = \alpha[T](1 - r) - \beta r \tag{1}$$

where $r(t)$ denotes the fraction of postsynaptic receptors bound to the neurotransmitter at time, t, $[T]$ is the neurotransmitter concentration, and α and β are the forward and backward rates for transmitter binding. Assuming receptor binding directly gates the opening of an associated ion channel, the resulting synaptic current can be described as [33]:

$$I_{syn} = \bar{g}_{syn} r(t)(V_{syn}(t) - E_{syn}) \tag{2}$$

where $\bar{g}_{syn}$ is the maximal synaptic conductance, $V_{syn}(t)$ is the postsynaptic potential and E_{syn} is the synaptic reversal potential. For the simulations, all synaptic parameters were set to values that gave the best fit to whole-cell recorded synaptic currents (see [33]). Parameters for AMPA synapses: $\alpha = 1.1 \times 10^6\ M^{-1}s^{-1}$, β = 190 s^{-1}, and E_{AMPA}=0mV. Parameters for $GABA_A$ receptors: $\alpha = 5 \times 10^6\ M^{-}s^{-}$, β= 180 s^{-1}, and E_{GABAA}= −80 mV. Synaptic plasticity was simulated by adapting the maximal synaptic conductance $\bar{g}_{AMPA}$ for recurrent excitatory

synapses onto both excitatory neurons and GABAergic interneurons according to the learning rules described in the text. The inhibitory synapses themselves were not adapted because evidence is currently lacking for their plasticity. We therefore used the following fixed values for $\bar{g}_{GABAA}$(in μS): 0.05 for mutual inhibition between the two chains and 0.016 for recurrent inhibitory connections within a chain for the simulations in Fig 3. Synaptic plasticity for connections onto excitatory neurons was simulated by changing maximal synaptic conductance $\bar{g}_{AMPA}$ by an amount equal to $\Delta\bar{g}_{AMPA} = \alpha\,(P_{t+\Delta t} - P_t)$ for each presynaptic spike at time t, where P_t denotes the postsynaptic membrane potential at time t (synapses onto inhibitory neurons were modified by an amount equal to $-\Delta\bar{g}_{AMPA}$) This simulates a temporal difference learning rule for prediction and results in asymmetric learning windows similar to those observed in physiological experiments (see [29] for more details). The synaptic conductance was adapted whenever the absolute value of;$\Delta\bar{g}_{AMPA}$ exceeded 10 mV with the gain α in the range 0.02–0.03 μS/V. The maximum value attainable by a synaptic conductance was set equal to 0.03 μS This phenomenological model of synaptic plasticity approximates the effects of known biophysical mechanisms such as calcium-dependent and NMDA (N-methyl-D-aspartate) receptor-dependent induction of long-term potentiation (LTP) and depression (LTD) (see [69] for a more detailed biophysical implementation).

Acknowledgments

This work was supported by the Alfred P Sloan Foundation, NIH, and Howard Hughes Medical Institute. We are grateful to Margaret Livingstone for her collaboration and for providing the data in Fig 7*b*. We also thank Dmitri Chklovskii, David Eagleman, and Christian Wehrhahn for comments and suggestions.

References

1. Hubel DH, Wiesel TN. Receptive fields and functional architecture of monkey striate cortex. Journal of Physiology (London) 1968;195:215–243. [PubMed: 4966457]
2. Hubel DH, Wiesel TN. Receptive fields, binocular interaction, and functional architecture in the cat's visual cortex. Journal of Physiology (London) 1962;160:106–154. [PubMed: 14449617]
3. Ferster D, Chung S, Wheat H. Orientation selectivity of thalamic input to simple cells of cat visual cortex. Nature 1996;380:249–252. [PubMed: 8637573]
4. Reid RC, Alonso JM. The processing and encoding of information in the visual cortex. Curr Opin Neurboiol 1996;6(4):475–480.
5. Ferster D, Lindstrom S. An intracellular analysis of geniculocortical connectivity in area 17 of the cat. Journal Physiol (Lond) 1983;342:181–215. [PubMed: 6631731]
6. Henry G, Mustari M, Bullier J. Different geniculate inputs to B and C cells of cat striate cortex. Exp Brain Research 1983;52:179–189.
7. LeVay S, Gilbert C. Laminar patterns of geniculocortical projections in the cat. Brain Research 1976;113:1–19. [PubMed: 953720]
8. Singer W, Tretter F, Cynader M. Organization of cat striate cortex: a correlation of receptive-feld properties with afferent and efferent connections. Journal Neurophysiol 1975;30:1080–1098.
9. Chose GM, Freeman RD, Ohzawa I. Local intracortical connections in the cat's visual cortex: postnatal development and plasticity. Journal Neurophysiol 1994;72:1290–1303.
10. Toyama K, Kimura M, Tanaka K. Organization of cat visual cortex as investigated by cross-correlation technique. Journal Neurophysiol 1981;46:202–214.
11. Alonso JM, Martinez LM. Functional connectivity between simple cells and complex cells in cat striate cortex. Nat Neurosci 1998;1(5):395–403. [PubMed: 10196530]
12. Burr DC, Morrone MC, Maffei L. Intra-cortical inhibition prevents simple cells from responding to textured visual patterns. Exp Brain Res 43(3–4):455–4581. [PubMed: 7262240]
13. Hammond P, MacKay DM. Differential responsiveness of simple and complex cells in cat striate cortex to visual texture. Exp Brain Res 1977;30(2–3):275–296. [PubMed: 598430]

14. Movshon JA. The velocity tuning of single units in cat striate cortex. Journal Physiol (Lond) 1975;249 (3):445–468. [PubMed: 1177101]
15. Malpeli JG, Lee C, Schwark HD, Weyand TG. Cat area 17.1. Pattern of thalamic control of cortical layers. Journal Neurophysiol 1986;56(4):1062–1073.
16. Archie KA, Mel BW. A model for intradendritic computation of binocular disparity. Nature Neurosci 2000;3(l):54–63. [PubMed: 10607395]
17. Mel BW, Ruderman DL, Archie KA. Translation-invariant orientation tuning in visual “complex” cells could derive from intradendritic computations. Journal Neuroscience 1998;18(11):4325–4334.
18. Livingstone MS. Mechanisms of direction selectivity in macaque V1. Neuron 1998;20:509–526. [PubMed: 9539125]
19. Anderson JC, Binzegger T, Kahana O, Martin KA, Segev I. Dendritic asymmetry cannot account for directional responses of neurons in visual cortex. Nature Neurosci 1999;2(9):820–824. [PubMed: 10461221]
20. Daw NW, Wyatt HJ. Kittens reared in a unidirectional environment: evidence for a critical period. Journal of Physiology 1976;257(1):155–170. [PubMed: 948048]
21. Humphrey AL, Saul AB. Strobe rearing reduces direction selectivity in area 17 by altering spatiotemporal receptive-field structure. Journal Neurophysiol 1998;80(6):2991–3004.
22. Roerig B, Kao JPY. Organization of intracortical circuits in relation to direction preference maps in ferret visual cortex. Journal of Neuroscience 1999;19(24):RC44. [PubMed: 10594088]
23. Markram H, Lubke J, Frotscher M, Sakmann B. Regulation of synaptic efficacy by coincidence of postsynaptic APs and EPSPs. Science 1997;275:213–215. [PubMed: 8985014]
24. Bi GQ, Poo MM. Synaptic modifications in cultured hippocampal neurons: Dependence on spike timing, synaptic strength, and postsynaptic cell type. Journal Neurosci 1998;18:10464–10472.
25. Levy W, Steward O. Temporal contiguity requirements for long-term associative potentiation/ depression in the hippocampus. Neuroscience 1983;8:791–797. [PubMed: 6306504]
26. Zhang LI, Tao HW, Holt CE, Harris WA, Poo MM. A critical window for cooperation and competition among developing retinotectal synapses. Nature 1998;395:37–44. [PubMed: 9738497]
27. Feldman D. Timing-based LTP and LTD at vertical inputs to layer II/III pyramidal cells in rat barrel cortex. Neuron 2000;27(45–56)
28. Abbott LF, Blum KI. Functional significance of long-term potentiation for sequence learning and prediction. Cereb Cortex 1996;6:406–416. [PubMed: 8670667]
29. Rao RPN, Sejnowski TJ. Spike-timing dependent Hebbian plasticity as temporal difference learning. Neural Computation. 2001 in press.
30. Rao RPN, Livingstone MS, Sejnowski TJ. Direction selectivity from predictive sequence learning in recurrent neocortieal circuits. Soc Neuro Abstr 1999;25:1316.
31. Rao, RPN.; Sejnowski, TJ. Advances in Neural Information Processing Systems. Vol. 12. Cambridge, MA: MIT Press; 2000. Predictive sequence learning in recurrent neocortieal circuits; p. 164-170.
32. Mainen ZF, Sejnowski TJ. Influence of dendritic structure on firing pattern in model neocortieal neurons. Nature 1996;382:363–366. [PubMed: 8684467]
33. Destexhe, A.; Mainen, ZF.; Sejnowski, TJ. Kinetic models of synaptic transmission. In: Koch, C.; Segev, I., editors. Methods in Neuronal Modeling. Cambridge, MA: MIT Press; 1998.
34. Song S, Miller KD, Abbott LF. Competitive Hebbian learning through spike-timing dependent synaptic plasticity. Nature Neuroscience 2000;3:919–926.
35. Bell C, Bodznick D, Montgomery J, Bastian J. The generation and subtraction of sensory expectations within cerebellum-like structures. Brain, Behavior and Evolution 1997;50(Suppl,1):17–31.
36. Movshon JA, Van Sluyters RC. Visual neural development. Annu Rev Psychol 1981;32:477–522. [PubMed: 7015996]
37. Miller, KD. Correlation-based models of neural development. In: Gluck, MA.; Rumelhart, DE., editors. Neuroscience and Connectionist theory. Hillsdale, NJ: Lawrence Erlbaum Associates; 1990. p. 267-353.
38. Sillito AM. The contribution of inhibitory mechanisms to the receptive field properties of neurones in the striate cortex of the cat. Journal Physiol (Lond) 1975;250(2):30–329.

39. Nelson S, Toth L, Sheth B, Sur M. Orientation selectivity of cortical neurons during intracellular blockade of inhibition. Science 1994;265:774–777. [PubMed: 8047882]
40. Chance FS, Nelson SB, Abbott LF. Complex cells as cortically amplified simple cells. Nature Neuroscience 1999;2:277–282.
41. Tootell RB, Switkes E, Silverman MS, Hamilton SL. Functional anatomy of macaque striate cortex. II. Retinotopic organization. Journal Neurosci 1988;8(5):1531–1568.
42. Van Essen, DC. Functional organization of primate visual cortex. In: Peters, A.; Jones, EG., editors. Cerebral Cortex. 3. New York, NY: Plenum; 1985. p. 259-329.
43. Berry MJ, Brivanlou IH, A-Jordan T, Meister M. Anticipation of moving stimuli by the retina. Nature 1999;398:334–338. [PubMed: 10192333]
44. Feidler JC, Saul AB, Murthy A, Humphrey AL. Hebbian learning and the development of direction selectivity: the role of geniculate response timings. Network: Computation in Neural Systems 1997;8:195–214.
45. Wimbauer S, Wenisch OG, Miller KD, van Hemmen JL. Development of spatiotemporal receptive fields of simple cells: I Model Formulation. Biological Cybernetics 1997;77:453–461. [PubMed: 9433756]
46. Emerson, RC.; Citron, MC.; Felleman, DJ.; Kaas, JH. A proposed mechanism and site for cortical direction selectivity. In: Rose, D.; Dobson, VG., editors. Models of the Visual Cortex. New York, NY: Wiley; 1985. p. 420-431.
47. Koch, C.; Poggio, T. The synaptic veto mechanism: does it underlie direction and orientation selectivity in the visual cortex?. In: Rose, D.; Dobson, VG., editors. Models of the Visual Cortex. New York, NY: Wiley; 1985. p. 408-419.
48. Maex R, Orban GA. Model circuit of spiking neurons generating directional selectivity in simple cells. Journal Neurophysiol 1996;75(4):1515–1545.
49. Mineiro P, Zipser D. Analysis of direction selectivity arising from recurrent cortical interactions. Neural Computation 1998;10(2):353–371. [PubMed: 9472486]
50. Suarez H, Koch C, Douglas R. Modeling direction selectivity of simple cells in striate visual cortex with the framework of the canonical microcircuit. Journal Neurosci 1995;15(10):6700–6719.
51. Adelson EH, Bergen J. Spatiotemporal energy models for the perception of motion. Journal Opt Soc Am A 1985;2(2):284–299. [PubMed: 3973762]
52. Emerson RC, Bergen JR, Adelson EH. Directionally selective complex cells and the computation of motion energy in eat visual cortex. Vision Research 1992;32(2):203–218. [PubMed: 1574836]
53. Mehta MR, Barnes CA, McNaughton BL. Experience-dependent, asymmetric expansion of hippocampal place fields. Proc Natl Acad Sci, USA 1997;94:8918–8921. [PubMed: 9238078]
54. Mehta, MR.; Wilson, M. From hippocampus to V1: Effect of LTP on spatiotemporal dynamics of receptive fields. In: Bower, J., editor. Computational Neuroscience; Trends in Research 1999. Amsterdam: Elsevier Press; 2000.
55. Gerstner W, Kempter R, van Hemmen JL, Wagner H. A neuronal learning rule for sub-millisecond temporal coding. Nature 1996;383(76–81)
56. Stuart GJ, Sakmann B. Active propagation of somatic action potentials into neocortieal pyramidal cell dendrites. Nature 1994;367:69–72. [PubMed: 8107777]
57. Abbott LF, Varela JA, Sen K, Nelson SB. Synaptic depression and cortical gain control. Science 1997;275:220–224. [PubMed: 8985017]
58. Thomson AM, Deuchars J. Temporal and spatial properties of local circuits in neocortex. Trends Neurosci 1994;17(3):119–126. [PubMed: 7515528]
59. Tsodyks MV, Markram H. The neural code between neocortieal pyramidal neurons depends on neurotransmitter release probability. Proc Natl Acad Sci USA 1997;94(2):719–723. [PubMed: 9012851]
60. Barlow H. Cerebral predictions. Perception 1998;27:885–888. [PubMed: 10209631]
61. Daugman JG, Downing CJ. Demodulation, predictive coding, and spatial vision. Journal Opt Soc Am A 1995;12:641–660.
62. Minai, AA.; Levy, W. Sequence learning in a single trial. Proceedings of the 1993 INNS World Congress on Neural Networks II; Erlbaum: New Jersey; 1993. p. 505-508.

63. Montague PR, Sejnowski TJ. The predictive brain: Temporal coincidence and temporal order in synaptic learning mechanisms. Learning and Memory 1994;1:1–33. [PubMed: 10467583]
64. Mumford, D. Neuronal architectures for pattern-theoretic problems. In: Koch, C.; Davis, JL., editors. Large-Scale Neuronal Theories of the Brain. Cambridge, MA: MIT Press; 1994. p. 125-152.
65. Rao RPN, Ballard DH. Dynamic model of visual recognition predicts neural response properties in the visual cortex. Neural Computation 1997;9(4):721–763. [PubMed: 9161021]
66. Rao RPN, Ballard DH. Predictive coding in the visual cortex: A functional interpretation of some extra-classical receptive field effects. Nature Neuroscience 1999;2(1):79–87.
67. Schultz W, Dayan P, Montague PR. A neural substrate of prediction and reward. Science 1997;275:1593–1598. [PubMed: 9054347]
68. Koch, C. Biophysics of Computation: Information Processing in Single Neurons. New York: Oxford University Press; 1999.
69. Sehn W, Markram H, Tsodyks M. An algorithm for modifying neurotransmitter release probability based on pre- and postsynaptic spike timing. Neural Computation 2001;13(1):35–67. [PubMed: 11177427]

Biographies

Terrence Sejnowski, PhD, is a Howard Hughes Medical Institute Investigator, Professor and Director of the Computational Neuro biology Laboratory at The Salk Institute. He is also Professor of Biology and Adjunct Professor of Physics, Neurosciences, Psychology, Cognitive Science, Electrical and Computer Engineering, and Computer Science and Engineering at UCSD, where he is Director of the Institute for Neural Computation and Director of training programs in Computational Neurobiology and Cognitive Neuroscience. The goal of his research is to build linking principles from brain to behavior using computational models, and a combination of theoretical and experimental approaches ranging from the biophysical to the systems level. He is founding Editor of “Neural Computation” and President of the Neural Information Processing Systems (NIPS) Foundation. He is a past recipient of the Presidential Young Investigator Award, and was Wiersma Visiting Professor of Neurobiology and a Sherman Fairchild Distinguished Scholar at the California Institute of Technology where he continues as a part-time Visiting Professor. He is a Fellow of the IEEE and has received the Pioneer Award from the IEEE Neural Network Society.

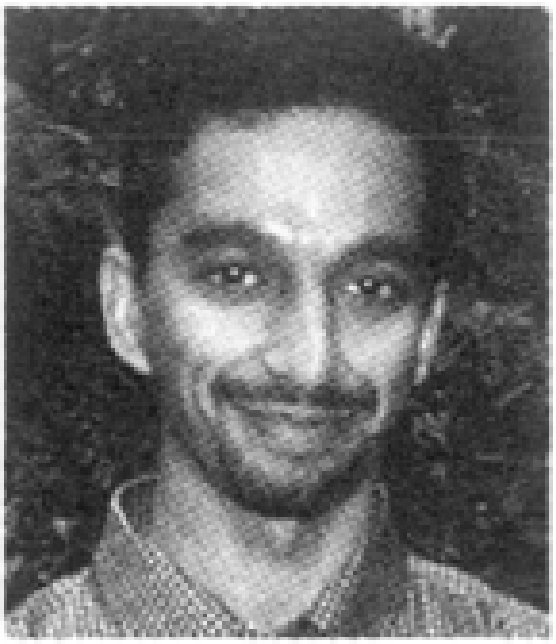

Rajesh P N Rao completed his high school in Hyderabad, India in 1988 and graduated summa cum laude in 1992 with bachelor's degrees in Computer Science and Mathematics from Angelo State University in Texas. He received his M S and PhD degrees in Computer Science from the University of Rochester, New York, and was an Alfred P Sloan Postdoctoral Fellow in computational neuroscience from 1997–2000 at the Salk Institute for Biological Studies in La Jolla, California. He is currently an assistant professor in the Computer Science and Engineering department and in the Neurobiology and Behaviour program at the University of Washington, Seattle. He received a Sloan Research Fellowship for junior faculty in 2001, an NSF career award and a David and Lucile Packard Fellowship in 2002, and an ONR Young Investigator Award in 2003. His current research interests span the areas of computational neuroscience, machine learning, computer vision, robotics, and brain-computer interfaces.

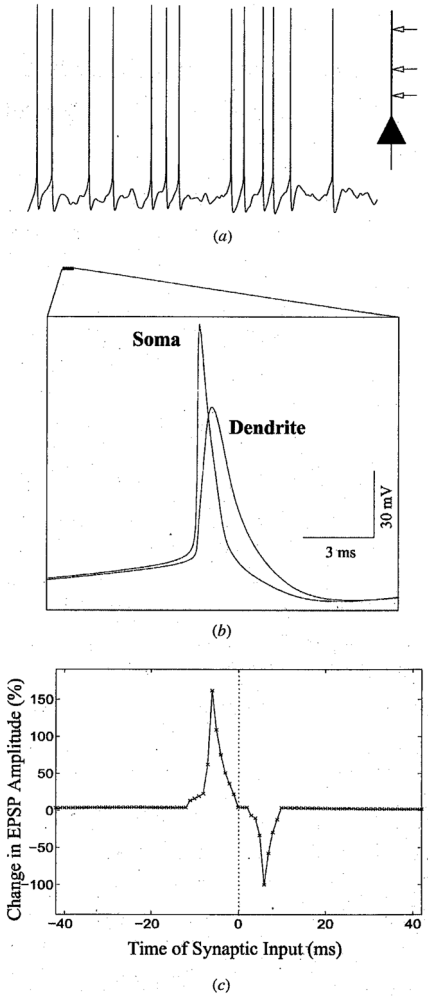

Fig 1.

Model Neocortical Neuron and Window of Synaptic Plasticity. (*a*) Response of the two-compartment model neuron to Poisson distributed excitatory and inhibitory synaptic inputs at random locations on the dendrite. (*b*) Example of a backpropagating action potential in the dendrite of the model neuron as compared to the corresponding action potential in the soma (enlarged from the initial portion of the trace in (*a*)). (*c*) Window for synaptic plasticity in the model neuron obtained by varying the delay between presynaptic stimulation and postsynaptic spiking (negative delays refer to cases where presynaptic stimulation occurred before the postsynaptic spike).

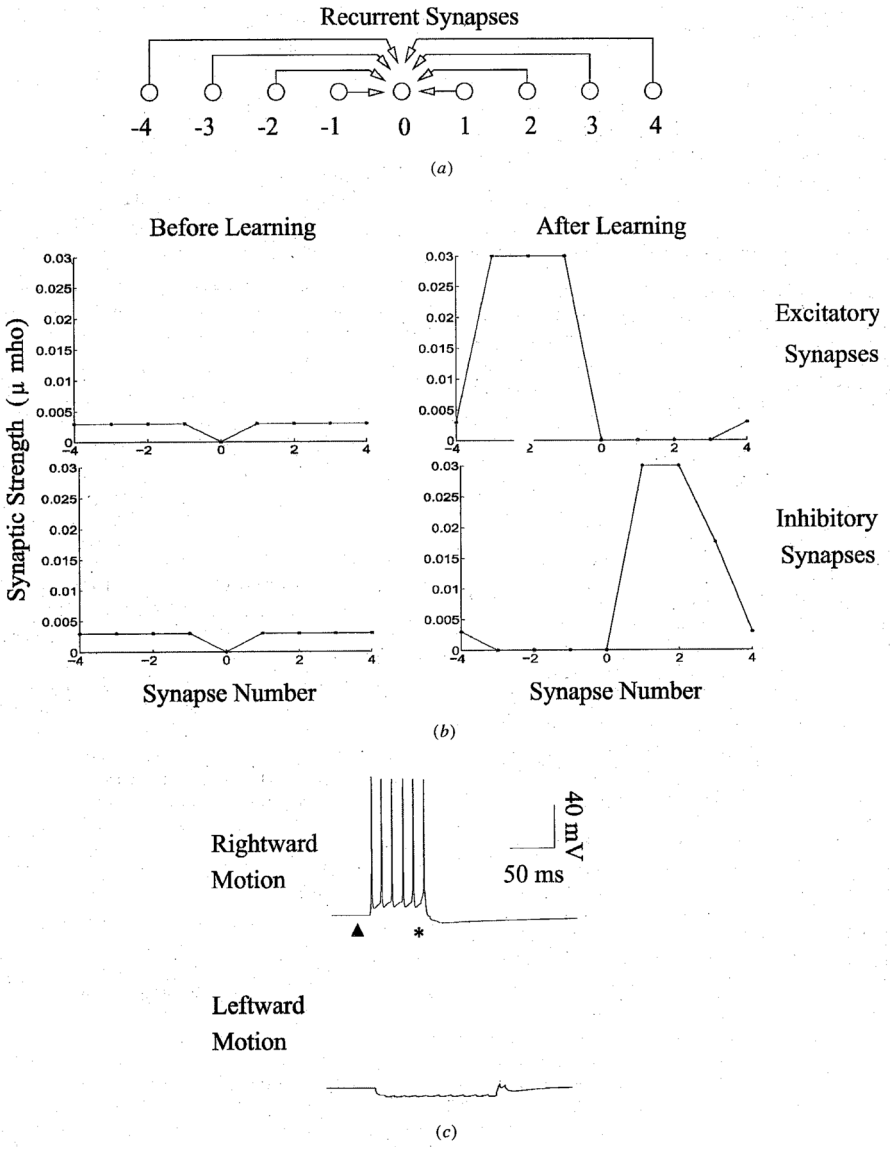

Fig 2.

Emergence of Direction Selectivity in the Model. (*a*) Schematic depiction of recurrent connections to a given neuron (labeled '0') from 4 preceding and 4 successor neurons in its chain. (*b*) Synaptic strength of recurrent excitatory and inhibitory connections to neuron 0 before and after learning. Note the symmetry in connections before learning and the asymmetry in connections after spike-timing dependent learning. Synapses were adapted during 100 trials of exposure to rightward moving stimuli. (*c*) Direction selective response of neuron 0 to rightward moving stimuli after learning. Due to recurrent excitation from preceding neurons, the neuron starts firing a few milliseconds before the expected arrival time of its input (marked by an asterisk). The dark triangle represents the time at which the input stimulus begins its rightward motion.

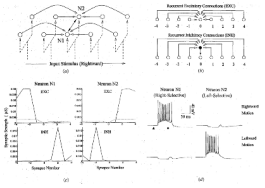

Fig 3.

Detecting Multiple Directions of Motion. (*a*) A model network consisting of two chain of recurrently connected neurons receiving retinotopic inputs. A given neuron receives recurrent excitation and recurrent inhibition(white-headed arrows) as well as inhibition (darkheaded arrows) from its counterpart in the other chain. (*b*) Recurrent connections to a given neuron (labeled '0') arise from 4 preceding and 4 succeeding neurons in its chain. Inhibition at a given neuron is mediated via a GABAergic interneuron (darkened circle). (*c*) Synaptic strength of recurrent excitatory (EXC) and inhibitory (INH) connections to neurons N1 and N2 before (dotted lines) and after learning (solid lines). Synapses were adapted during 100 trials of exposure to alternating leftward and rightward moving stimuli. (*d*) Responses of neurons N1 and N2 to rightward and leftward moving stimuli. After learning, neuron N1 has become selective for rightward motion (as have other neurons in the same chain) while neuron N2 has become selective for leftward motion. In the preferred direction, each neuron starts firing several milliseconds before the input arrives at its soma (marked by an asterisk) due to recurrent excitation from preceding neurons. The dark triangle represents the start of input stimulation in the network.

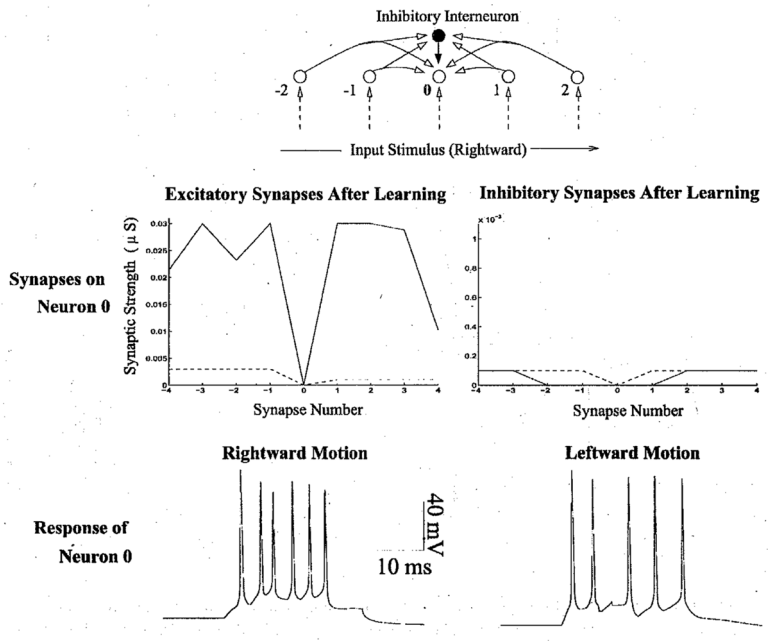

Fig 4.

The Effect of Rate-Based Hebbian Learning. The same network as in Fig 3, with identical initial conditions and input stimuli, was used to test the effects of rate-based learning. The top panel depicts the recurrent connections to a given neuron (labeled '0') in the two-chain network. The GABAergic interneuron is represented by the darkened circle. The middle panel represents the changes in synaptic strength as a result of rate-based Hebbian learning, which relies on correlations in pre- and postsynaptic spikes irrespective of their temporal order. Despite an initial asymmetry in the excitatory connections (dotted lines), ratebased Hebbian learning resulted in an approximately symmetric pattern of connections. As a result, the neurons in the two-chain network fail to exhibit direction selective responses (bottom panel).

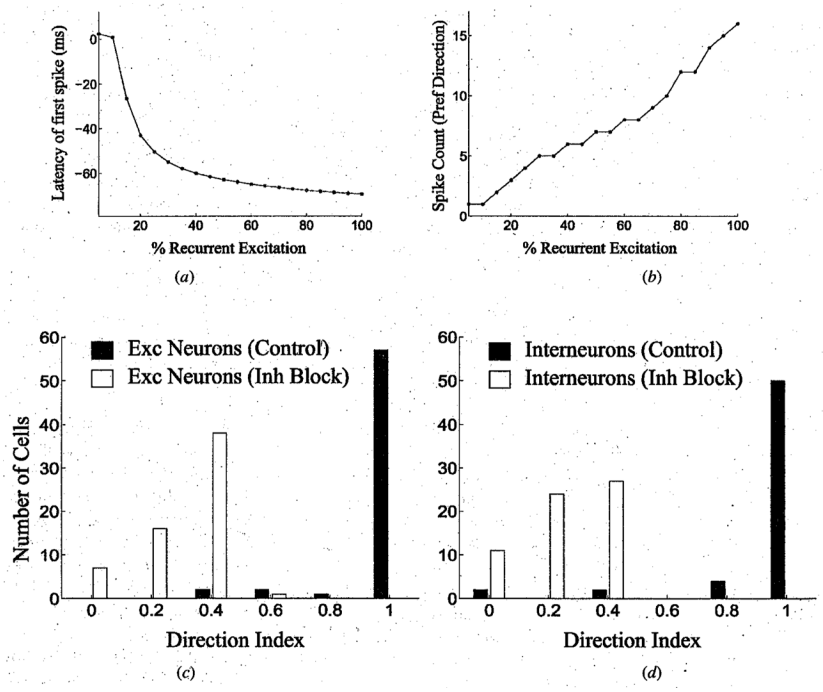

Fig 5.

The Role of Recurrent Excitation and Inhibition in Direction Selectivity. (*a*) & (*b*) Latency of the first spike and number of spikes elicited in an excitatory neuron in the preferred direction as a function of the strength of recurrent excitation in a model network (100% corresponds to the learned values of recurrent connection strength). The network comprised of two chains, each containing 35 excitatory neurons and 35 inhibitory interneurons (mutual inhibition between corresponding neurons in the two chains was mediated by a separate set of inhibitory neurons that were not plastic). (*c*) & (*d*) Distribution of direction selectivity in the network for excitatory and inhibitory interneurons respectively with GABAergic inhibition (Control) and without GABAergic inhibition (Inh Block) as measured by the direction index: 1 - (Non-Preferred Direction Response)/(Preferred Direction Response).

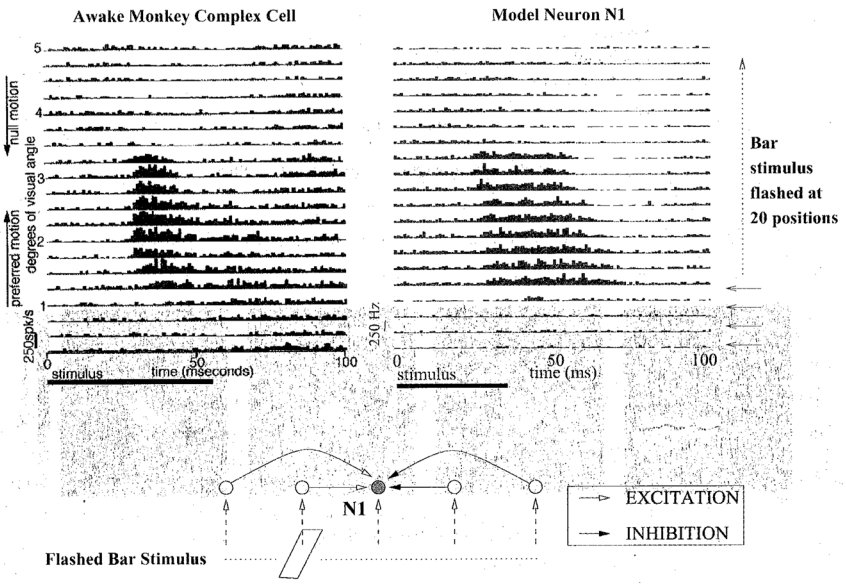

Fig 6.

Comparison of Monkey and Model Space-Time Response Plots to Single Flashed Bars. (Top, Left) Sequence of PSTHs obtained by flashing optimally oriented bars at 20 positions across the 5°-wide receptive field (RF) of a complex cell in alert monkey V1 (from [18]). The cell's preferred direction is from the part of the RF represented at the bottom towards the top. Flash duration = 56 ms; inter-stimulus delay = 100 ms; 75 stimulus presentations. (Top, Right) PSTHs obtained' from a model neuron after stimulating the chain of neurons at 20 positions to the left and right side of the given neuron. The lower PSTHs represent stimulations on the preferred side while upper PSTHs represent stimulations on the null side. (Bottom pane1) Interpretation of the space-time plots in the model. Bars flashed on the left (preferred) side of the recorded cell (shaded) cause progressively greater excitation as the stimulation site approaches the recorded cell's location. Bars flashed to the right of the cell cause inhibition due to the predominantly inhibitory connections that develop on the right (null) side during learning.

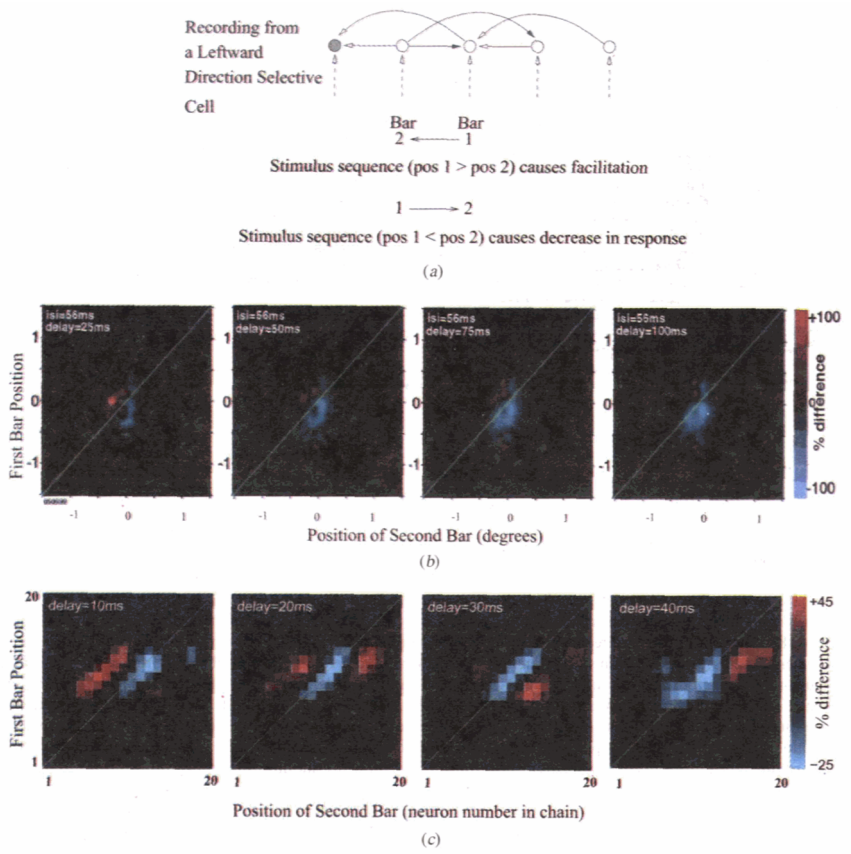

Fig 7.

Two-Bar Interactions. (*a*) Model predictions for sequential presentation of two optimally oriented bars. Dark arrowheads represent inhibitory connections. Facilitation is predicted when spatial position of bar 1 is greater than that of bar 2 (relative motion in the preferred direction); a reduction in response is expected when position of bar 2 is greater than that of bar 1 due to recruitment of inhibition. (*b*) Sequential two-bar interaction maps for a direction selective complex cell in awake monkey V1. The maps show the percent difference in response after subtracting the average responses to the individual bars from the cell's two bar response. The four plots represent the cell's response to the two bar sequence at delays of 25 ms, 50 ms, 75 ms, and 100 ms respectively after the onset of bar 2. The inter-stimulusinterval (i.s.i.) between bar 1 and bar 2 was 56 ms. (*c*) Two-bar interaction maps for the model network. Note the slightly different scale bar for model data as compared to the experimental data. Both model and experimental data show qualitatively similar sequential interactions consistent with the expectations in (*a*), namely, facilitation (red) for spatial points above the diagonal (bar 1 position > bar 2 position) and a reduction in response (blue) for points close to and below the diagonal.